Calculations with spectroscopic accuracy for the ground configuration ($3d^9$) forbidden transition in Co-like ions

X. L. Guo,[1,2,*] R. Si,[1,2] S. Li,[1,2] M. Huang,[1,2] R. Hutton,[1,2] Y. S. Wang,[1,2] C. Y. Chen,[1,2,†] Y. M. Zou,[1,2] K. Wang,[3,4] J. Yan,[4,5] C. Y. Li,[4] and T. Brage[6,‡]

[1]*Shanghai EBIT Laboratory, Modern Physics Institute, Fudan University, Shanghai 200433, China*

[2]*The Key Laboratory of Applied Ion Beam Physics, Ministry of Education, Fudan University, Shanghai 200433, China*

[3]*Hebei Key Laboratory of Optic-Electronic Information and Materials, The College of Physics Science and Technology, Hebei University, Baoding 071002, China*

[4]*Institute of Applied Physics and Computational Mathematics, Beijing 100088, China*

[5]*Center for Applied Physics and Technology, Peking University, Beijing 100871, China*

[6]*Division of Mathematical Physics, Department of Physics, Lund University, Sweden*

(Received 11 July 2015; revised manuscript received 28 October 2015; published 20 January 2016)

We present systematic and large-scale calculations for the fine-structure energy splitting and transition rate between the $3d^9\ ^2D_{3/2,5/2}$ levels of Co-like ions with $28 \leqslant Z \leqslant 100$. Two different fully relativistic approaches are used, based on the multiconfiguration Dirac-Hartree-Fock (MCDHF) theory and the relativistic many-body-perturbation theory (RMBPT). Especially the former gives results of similar accuracy as experiments for a large range of ions. Our calculations are therefore accurate enough to probe Breit and quantum-electro-dynamic effects. To obtain spectroscopic accuracy, we show that it is important to include deep core-valence correlation, down to and including the $n = 2$ shell. We estimate that the uncertainties of our wavelengths are within the uncertainty of experiments, i.e., 0.02%. We also show that the frequently used flexible atomic code has an inaccurate treatment of the self-energy (SE) contribution and of the $M1$-transition properties for lower-Z ions. After correcting for the SE calculation, the resulting RMBPT transition energies are in good agreement with the MCDHF ones, especially for the high-Z end of the Co-like sequence.

DOI: 10.1103/PhysRevA.93.012513

I. INTRODUCTION

Electric dipole forbidden transitions play a vital role in the diagnostics of astrophysical and laboratory plasma (e.g., [1–4]), since their intensities are in general sensitive to the density and temperature of the plasma. They have also been proposed as the basis of optical atomic clocks of exceptional accuracy [5], as well as to study the variation of the fine-structure constant with time [6]. Recently such lines have also been proposed to be used for accurate tests of the treatment of quantum-electro-dynamic (QED) effects in many-body theories [7,8].

In this paper we will focus on transitions between fine-structure levels belonging to ground configurations. These are often dominated by magnetic dipole ($M1$) transitions, and one historical example is the strongest corona line at 530.3 nm, identified as the $3s^2 3p\ ^2P_{3/2}$-$^2P_{1/2}$ fine-structure transition in Fe XIV by Edlén [9].

In the past decades there have been many accurate theoretical predictions and measurements for highly charged ions with one valence electron (e.g., Refs. [8,10–25]). Since these systems are relatively simple, the accuracy of the calculations is high enough to allow for tests of higher-order QED effects [12–15].

Forbidden transitions within the ground configuration consisting of full subshells, except for one with a hole or vacancy (e.g., $1s^2 2s^2 2p^5$), are similar to the one-valence-electron system, but should involve more complex correlation. In the present work we focus on the cobaltlike system for $28 \leqslant Z \leqslant 100$, which has the ground configuration of $3d^9$. The atomic Co ground configuration is $3d^7 4s^2$, which is not considered in this work. These systems have been investigated both experimentally and theoretically for many years [26–47]. Special interest has been given to the ground-state fine-structure line ($3d^9\ ^2D_{3/2}$-$^2D_{5/2}$) [35–46] which is dominated by $M1$ decay. Up to now, the $M1$ transition line has been directly observed for only seven cobaltlike ions, from Zr^{13+} to Mo^{15+} [37,38], Hf^{45+} to W^{47+}, and Au^{52+} [39–42], with an uncertainty in wavelength to within 0.02%. On the theoretical side, investigations [41–47] mainly focused on the energy structure, without systematic calculations of other transition properties, such as rates or line strengths.

In a recent study [47], we presented the results of calculations for forbidden lines within the $3d^k (k = 1\text{–}9)$ ground configurations for four high-Z ($Z = 72, 73, 74, 79$) ions, using the relativistic many-body perturbation (RMBPT) theory based on the flexible atomic code (FAC) [48–50]. The calculated wavelengths agree with the experimental values [41,42] to within 0.2%, which is a clear improvement over previous theoretical results [41–46]. The differences between these previous theoretical results and observations are in the range of 0.1 to 3%. In Ref. [47], we also dramatically removed the systematic underestimation (overestimation) for shorter (longer) wavelengths which existed in previous calculations [41–46]. For the cobaltlike ions the agreement between experiments and RMBPT calculations was found to be about

*Present address: Department of Radiotherapy, Shanghai Changhai Hospital,Second Military Medical University, Shanghai 200433, China.

†Author to whom correspondence should be addressed: chychen@fudan.edu.cn

‡Author to whom correspondence should be addressed: tomas.brage@fysik.lu.se

0.1%, which in spite of being impressive still is substantially larger than the stated experimental uncertainty.

Highly accurate results for forbidden line wavelengths were recently reported [23,24] from fully relativistic multiconfiguration Dirac-Hartree-Fock (MCDHF) calculations, by using the GRASP2K package [51,52]. The close to spectroscopic accuracy of these calculations for the silverlike isoelectronic sequence, with a ground configuration of one open singly occupied $4f$ subshell, could be achieved by a systematic inclusion of deep core-valence correlation. While the silverlike sequence represents one-electron ($4f$) systems, outside closed subshells, this paper investigates if it is possible to achieve a similar accuracy for single-vacancy ground configurations. For theoretical calculations, high accuracy is required, to be able to identify the single transition in the visible spectral region, as was discussed for the silverlike sequence [24]. High accuracy also opens up the possibility to measure the higher-order relativistic (Breit) and QED effects, in what we will label BQ contributions.

II. THEORETICAL APPROACH

We report on results from two different computational methods, MCDHF in the form of the GRASP2K package [52] and RMBPT based on the FAC code [49]. Both are described in detail elsewhere, so we here only give an outline of these methods. In both methods, we start by defining the Dirac-Coulomb Hamiltonian as

$$H_{\rm DC} = \sum_{j=1}^{N}[\alpha_j \cdot p_j + \beta_j c^2 + V_{\rm nuc}(r_j)] + \sum_{j<k}\frac{1}{r_{jk}} \qquad (1)$$

where $V_{\rm nuc}(r_j)$ is the nuclear potential $-\frac{Z}{r_j}$, corrected for a Fermi-nuclear potential, and we use standard notations.

A. MCDHF

In the MCDHF method, the ion is represented by an atomic state function $\Psi(\gamma J)$, which in turn is a linear combination of a number of configuration state functions (CSFs):

$$\Psi(\gamma J) = \sum_i c_i \Phi(\gamma_i J). \qquad (2)$$

The CSFs, $\Phi(\gamma_i J)$, are constructed as liner combinations of single-electron Dirac orbitals, according to the well-known rules of symmetry (parity and angular momenta) [53]. The coefficients c_i and the radial parts of the Dirac orbitals are determined by solving the MCDHF equations which are derived by using the variational approach, within the self-consistent-field method. In the variational part of the calculations we include the Dirac-Coulomb Hamiltonian, defined above.

One main advantage of the multiconfigurational method is the fact that correlation can be included in a systematic way, by using the notion of an active set (AS) of orbitals, that are in turn used to generate CSFs [54]. We classify different types of correlation, by defining the outermost and open $3d$ subshells as valence electrons, while the rest are core subshells. The correlation between the valence electrons is defined as valence-valence (VV) correlation, and the correlation between the valence electrons and core electrons is labeled core-valence (CV), while the correlation between the core electrons is referred to as core-core (CC) correlation. The details of this approach are described elsewhere [23].

Once we obtain a set of radial orbitals, we perform relativistic configuration interaction (RCI) calculations. In the RCI calculations higher-order relativistic effects can be included in the form of the transverse photon interaction described by the Hamiltonian:

$$H_{\rm TP} = -\sum_{j<k}\left[\frac{\alpha_j\cdot\alpha_k\cos(\omega_{jk}r_{jk}/c)}{r_{jk}} + (\alpha_j\cdot\nabla_j)(\alpha_k\cdot\nabla_k)\frac{\cos(\omega_{jk}r_{jk}/c)-1}{\omega_{jk}^2 r_{jk}}\right]. \qquad (3)$$

The photon frequency ω_{jk} used by the RCI program in calculating the matrix elements of the transverse photon interaction is derived from the difference in the diagonal Lagrange multipliers of the associated orbitals. Since this is not well defined for correlation orbitals, we follow the established approach and use the low-frequency limit $\omega_{ij} \to 0$. Then $H_{\rm TP}$ reduces to

$$H_{\rm Breit} = \sum_{j<k} B_{jk} \qquad (4)$$

where

$$B_{jk} = \frac{1}{2r_{jk}}\left[(\alpha_j\cdot\alpha_k) + \frac{(\alpha_j\cdot\omega_{jk})(\alpha_k\cdot\omega_{jk})}{r_{jk}^2}\right]. \qquad (5)$$

To represent the QED corrections, we include hydrogenlike approximation of the self-energy (SE) and vacuum polarization (VP) [55,56].

B. RMBPT

The RMBPT calculations are based on the FAC package [48–50] described in more detail elsewhere [47,57–60]. The method is based on an approximation of the Dirac-Coulomb-Breit (DCB) Hamiltonian $H_{\rm DCB}$ [61]

$$H_{\rm DCB} = H_{\rm DC} + H_{\rm Breit} \qquad (6)$$

through the introduction of a one-electron model potential $U_j(r_j)$. This is defined as a one-electron local central field potential, including the screening effect of all other electrons. It is derived from a Dirac-Fock-Slater self-consistent-field calculation, minimizing the weighted mean energy of a set of configurations. In practice this means that the $H_{\rm DCB}$ operator is split into a zeroth-order model Hamiltonian H_0 and a perturbation Hamiltonian V, according to

$$H_0 = \sum_{j=1}^{N}[\alpha_j\cdot p_j + \beta_j c^2 + V_{\rm nuc}(r_j) + U_j(r_j)],$$
$$V = \sum_j\left[\sum_{k<j}\left(\frac{1}{r_{jk}} + B_{jk}\right) - U_j(r_j)\right], \qquad (7)$$

which is the basis for the perturbation expansion in the RMBPT method.

The key feature of the RMBPT theory is that it splits the Hilbert space of the full Hamiltonian into two subspaces spanned by the included configurations: a model space, M, and the orthogonal space, N. A limited number of configurations span the M subspace, where the correlation effects are exactly accounted for, by including all orders of configuration interaction expansion, while interaction between M and N is taken into account with the second-order perturbation method.

In the present work, the M space is spanned by the states belonging to the main configuration $3d^9$, while the N space is created by single and double excitations from these. Several small corrections to the Hamiltonian have been included in the calculations, namely, finite nuclear size, nuclear recoil, vacuum polarization, and electron self-energy, though the nuclear size and specific mass contributions were negligible. These are all taken into account with standard procedures of atomic structure theory, in a similar fashion to the methods in GRASP2K [51,52].

III. MCDHF CALCULATIONS

A. Active sets of orbitals

To reach high accuracy, we use a systematic approach based on the idea of excitation from a reference set into an AS of orbitals, according to some restrictions. The resulting set of CSFs spans a restrictive active space [62]. By increasing the AS step by step, we can investigate the convergence of our calculations. We limit our approach to single and double excitations, since it has been shown that the contribution from triple and quadruple excitations is small [63]. The effect of high-l (h and i) orbitals on transition energies and rates has also been tested and found to be negligible.

We define our calculations from the following AS: we start with a single reference state of $3d^9\ ^2D_{3/2}$ and $^2D_{5/2}$ which is usually labeled as the Dirac-Fock (DF) calculation, but here we will use the notation AS_0 for this first approximation. We are then increasing the AS according to

$$\begin{aligned}
\mathrm{AS}_1 &= 3d + \{4s,4p,4d,4f\},\\
\mathrm{AS}_2 &= \mathrm{AS}_1 + \{5s,5p,5d,5f,5g\},\\
\mathrm{AS}_3 &= \mathrm{AS}_2 + \{6s,6p,6d,6f,6g\},\\
\mathrm{AS}_4 &= \mathrm{AS}_3 + \{7s,7p,7d,7f,7g\},\\
\mathrm{AS}_5 &= \mathrm{AS}_4 + \{8s,8p,8d,8f,8g\}.
\end{aligned}$$

1. Valence-valence correlation

In the valence-valence (VV) model, the Ar-like $1s^22s^2\ldots3p^6$ core was treated as an inactive core, and we only allow the $3d$ valence electron to be excited to the active set, giving $3d^7nln'l'$ where nl and $n'l'$ belong to the active set. To study the convergence of the fine-structure energy, we define $\Delta E_m = E_m(^2D_{3/2}) - E_m(^2D_{5/2})$, where m denotes energies from calculations with active set AS_m, $m = 0,\ldots,5$. We also introduce a convergence ratio between calculations using AS_m and AS_{m-1} as $(\Delta E_m - \Delta E_{m-1})/\Delta E_{m-1}$. The convergence trend of our valence-valence calculation is given in Fig. 1. It is clear that the convergence is fairly fast and that we could use the expansion with maximum $n = 7$ (AS_4) as defining the final results for lower Z ($Z = 28$–42), while for higher Z ($Z = 43$–100) the AS_3 results are sufficient. It is a fair estimate that the convergence of the VV calculations is within 0.01%, which is well within the experimental accuracy, estimated to be 0.03% for higher-Z Co-like ions.

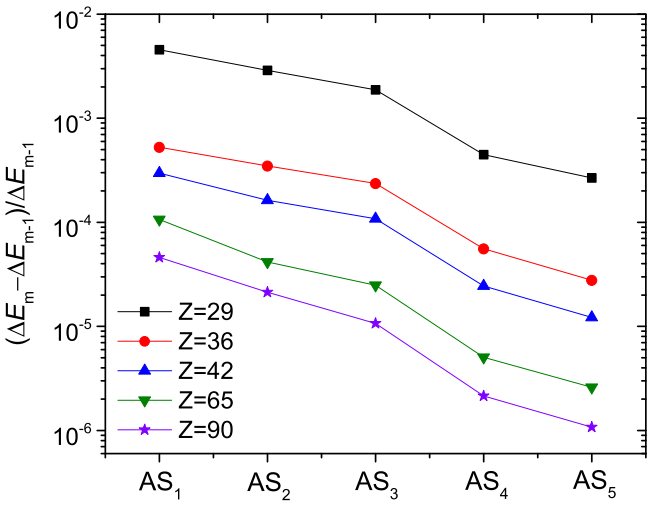

FIG. 1. Relative convergence of the $\Delta E_m = E_m(^2D_{5/2}) - E_m(^2D_{3/2})$ fine-structure energy as the size of the active set ASm of orbitals is increased in a layer-by-layer scheme in the VV model, for five different ions in the Co-like sequence.

2. Separate core-valence correlation

To explore the importance of different core correlation contributions, we start with what was labeled a separate approach for the CV correlation (SCV) in the recent investigation of silverlike ions [23,24]. The aim is to probe the influence of one core subshell at a time, on the fine structure of the ground term. In addition to the VV correlation described above, we include single excitation from one core subshell at a time. The effect of core valence correlation of subshell nl can then be defined as the difference between the computed fine structure with valence-valence and this core-valence correlation [$\Delta E_{\mathrm{SCV}}(nl)$] and the fine structure obtained when including only valence-valence correlation (ΔE_{VV}). This is shown in the top panel of Fig. 2, along the isoelectronic sequence. In the bottom panel we display the relative size of the contribution from core-valence correlation, compared to the fine structure with only valence correlation included. We include separate CV contributions from the $3p,3s,2p,2s$ subshells (the contribution from $1s$ is negligible, even when aiming for spectroscopic accuracy).

It is interesting to note that the contribution to the fine-structure splitting from the $2p$ subshell is larger than the one from $3p$. The two counteract one another all through the sequence. The contributions from the s subshells are considerably smaller than from the p subshells, albeit the contribution from $2s$ is larger than from $3s$. It is clear that the CV correlation from $2s$ cannot be ignored in high-accuracy calculation. As expected, the relative importance of the contributions from CV decrease with increasing nuclear charge.

It is an interesting result that the correlation contribution to the fine structure is significant from deep core subshells. This is in accordance with the situation for silverlike ions

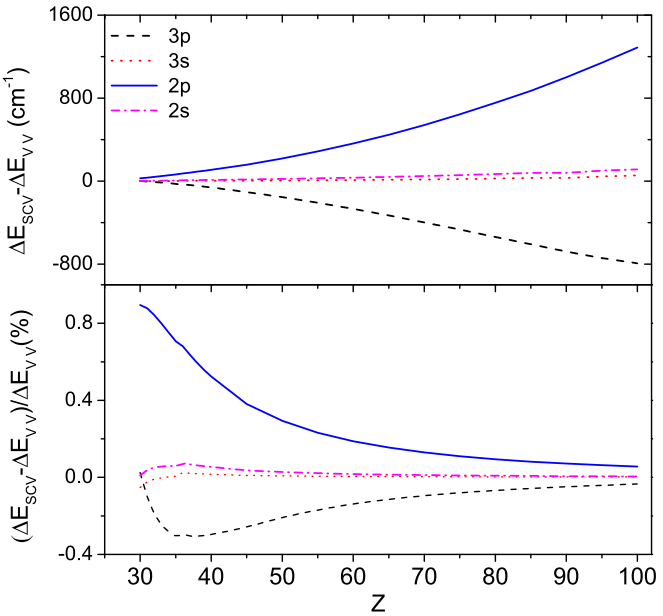

FIG. 2. CV contributions to the fine-structure splitting of $3d^2\ ^2D$. The top panel is for the absolute energy difference between the SCV and VV model for each core subshell (in cm^{-1}) and the bottom one is for the relative contribution in %.

[23,24] in which the inner core $3d$ showed a surprisingly large contribution to the fine structure within the ground term of $4d^{10}4f$.

3. *Separate core-core correlation*

When considering the core-core (CC) correlation, the size of the active space increases rapidly with the active set and therefore convergence is hard to achieve. By using a similar model to SCV, but allowing for double excitations from each core subshell separately, we defined a separate core-core correlation model. To investigate the contribution from core-core correlation for the cobaltlike system, we have checked the CC contributions for W^{47+}, and we find it is very small, around 0.003%. We therefore ignore the core-core correlation contributions.

4. *Full core-valence correlation*

After these more exploratory calculations, we define our final model as full core valence (FCV) by including both valence-valence correlation, through single and double excitations from the $3d$ core, as well as full core-valence correlation by single and double excitation involving one excitation from all core subshells (except $1s$) simultaneously. In Fig. 3 we give the total correlation contributions from the FCV model and the VV model, compared to the DF model, to the transition energy ΔE along the isoelectronic sequence. It is clear from this figure that the valence-valence correlation becomes relatively small and that the contribution to the fine structure from correlation is dominated by core-valence correlation for higher nuclear charges. The convergence of the final FCV calculations is within 0.02%, when using the same AS as for the VV model, which is again well within the experimental accuracy.

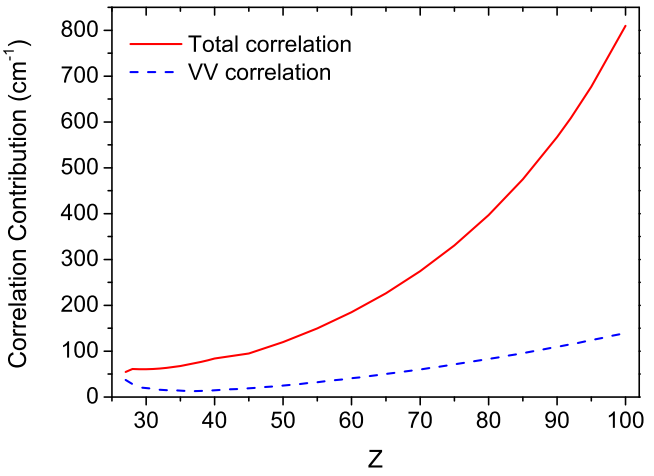

FIG. 3. Contribution to the fine-structure splitting of $3d^9\ ^2D$ from different types of correlation effects as a function of Z.

B. Breit and QED effects

After including valence-valence and core-valence correlation, the remaining discrepancy between our calculations and experimental results could be referred to as the BQ effect. These are estimated in the GRASP2K package, but only in an approximate fashion. For Breit interaction, as pointed out above, we use the low-frequency limit and for QED only approximate estimates of the SE and the VP. In Table I we report the results from our MCDHF calculations for different contributions to the fine-structure energy of $3d^9\ ^2D$ for some selected ions along the cobaltlike sequence.

It is clear that the Breit interaction is the dominating correction to the fine-structure energy for all ions. The contribution from SE is about 10% of the Breit contributions, while the VP is negligible for all ions.

IV. RMBPT CALCULATIONS

For comparison and support to our more elaborate MCDHF calculations, we also performed RMBPT calculations based on the FAC code [48–50] from Zn^{3+} to Fm^{73+} ions.

In this RMBPT calculation, all three kinds of electron-correlations are included, namely, valence-valence, core-valence, and core-core correlations. The perturbation expansion, up to second order, only includes configurations formed by single and double excitations from the reference $3d^9$. For the single excitations, we included configurations with one electron with principal quantum number $n \leqslant 125$. For double excitations, configurations with one electron with $n \leqslant 65$ and a second one with $n \leqslant 125$ are included. The maximum orbital quantum number was always set to $l_{\max} = 15$. To estimate the accuracy and the convergence of our calculations, we systematically increased the expansion defining the N space step by step, as discussed by Fei *et al.* [57] for Cd-like W^{26+}. We estimate the convergence to be within one part in a million.

TABLE I. Contributions to transition energies $\Delta E(^2D)$ (in cm^{-1}) from different effects of MCDHF and RMBPT methods. The different acronyms represent Dirac-Fock (DF), valence-valence (VV), core-valence (CV), Dirac-column (DC), Breit interaction (Breit), self-energy (SE), and vacuum polarization (VP). And the total contribution is marked as Tot. The SE0 and SE1 of the RMBPT represent the self-energy without and with $j \geqslant 5/2$ contribution, the former marked with brackets.

		MCDHF								RMBPT					
Z	Ion	DF	VV	CV	DC	Breit	SE	VP	Tot	DC	Breit	[SE0]	SE1	VP	Tot
30	Zn^{3+}	2875	20	36	2936	−184	4	0	2758	2716	−179	[2]	4	0	2541
35	Br^{8+}	8932	14	47	9000	−429	13	0	8584	8938	−429	[6]	13	0	8522
40	Zr^{13+}	20834	15	60	20918	−817	31	0	20132	20884	−822	[15]	31	−1	20093
45	Rh^{18+}	41451	19	76	41546	−1387	64	−1	40222	41533	−1393	[31]	66	−1	40205
50	Sn^{23+}	74229	25	95	74349	−2174	119	−1	72293	74345	−2183	[55]	121	−2	72281
55	Cs^{28+}	123217	32	117	123366	−3222	203	−3	120344	123369	−3232	[90]	205	−3	120338
60	Nd^{33+}	193087	41	144	193272	−4578	325	−4	189015	193283	−4588	[139]	327	−5	189016
65	Tb^{38+}	289171	50	177	289398	−6295	494	−7	283590	289415	−6301	[202]	496	−9	283600
70	Yb^{43+}	417485	60	215	417760	−8428	722	−12	410042	417783	−8429	[279]	722	−15	410060
75	Re^{48+}	584767	71	260	585098	−11041	1020	−19	575058	585128	−11033	[369]	1017	−23	575087
80	Hg^{53+}	798514	83	314	798911	−14204	1402	−30	786079	798951	−14182	[468]	1393	−36	786125
85	At^{58+}	1067020	96	384	1067500	−17991	1881	−46	1051344	1067548	−17949	[570]	1864	−53	1051406
90	Th^{63+}	1399440	109	451	1400000	−22482	2473	−71	1379920	1400067	−22415	[662]	2442	−82	1380008
95	Am^{68+}	1805771	124	553	1806448	−27765	3192	−108	1781763	1806530	−27660	[730]	3140	−120	1781880
100	Th^{73+}	2296972	140	670	2297781	−33929	4056	−165	2267738	2297890	−33790	[730]	3970	−190	2267890

V. RESULTS AND DISCUSSION

We start by comparing in detail the results from our two calculations. In Table I we give the contributions from different effects in the two approaches for a selected number of ions, while in Fig. 4 we show the difference between the RMBPT and MCDHF values of predicted energy contributions (δE), from correlation effect, Breit interaction, and SE contribution. There are two important deviations between the two methods. First, for the low-Z end, the RMBPT method represents a less accurate treatment of correlation, differing by about 200 cm^{-1} from the MCDHF result for Zn^{3+}. The reason for this is most likely due to the approximate potential representing the electron-electron interactions [49]. In the RMBPT implementation, this is approximated by a local central potential and is derived from a Dirac-Fock-Slater self-consistent-field calculation, which minimizes the weighted mean energy of all relevant configurations, as mentioned above. In the MCDHF method, we use the nonlocal Dirac-Hartree-Fock potential. The second, and larger, deviation is for high Z where the two methods diverge in the prediction of the self-energy. We here use the standard setting in the FAC code (labeled SE0 in Table I and Fig. 4). The reason for this deviation is the fact that in the FAC code the SE correction is only included through the estimate of the effect of a strong Coulomb field for electron states with quantum numbers $n \leqslant 5$ and $j = 1/2,3/2$ [55,64,65], omitting the $j \geqslant 5/2$ contributions, which are included in MCDHF. We correct for this and get the results labeled SE1 in Table I and Fig. 4, in excellent agreement with the MCDHF results.

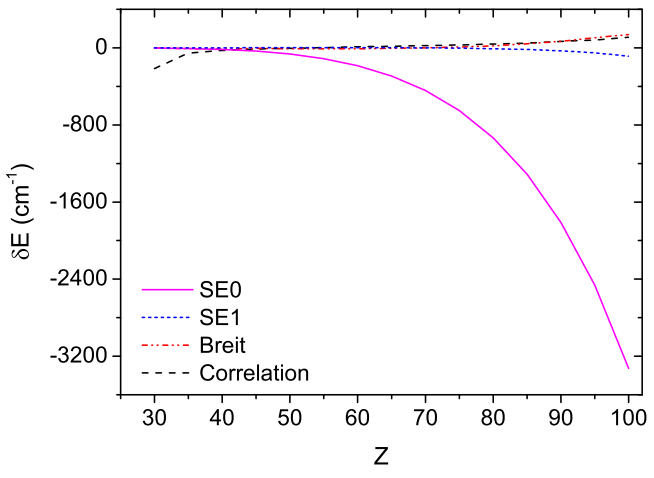

FIG. 4. Absolute differences in the predicted contributions to different relativistic effects from RMBPT and MCDHF calculations. SE0 and SE1 refer to standard, for FAC code, and corrected treatment of self-energy (see text), respectively.

We present our final results from MCDHF-FCV and RMBPT calculations in Tables II–IV and Fig. 5, where we also compare with other theories and experiments, when available.

In Table II, we give the transition energies $[\Delta E(^2D) = E(^2D_{5/2}) - E(^2D_{3/2})]$ for the whole sequence. The column marked "Expt.$_{\rm DIR}$" represents transition energies that are measured directly by observation of the $3d^9\,{}^2D_{3/2} \rightarrow {}^2D_{5/2}$ forbidden line [37–42]. "Expt.$_{\rm IND}$" represents indirect measurements, through transitions from higher excited terms [31–33,66]. The energies marked as "Semiemp." are determined either by interpolation or extrapolation of known experimental values or by semiempirical calculations [31,32,35].

In Fig. 5 we compare other results with our MCDHF calculations. It is clear that we have excellent agreement with the direct measurements, well within the experimental uncertainties of 0.02%. For indirect measurements, the agreement is good with two exceptions. First is the observation of Dy^{39+} ($Z = 66$), where the deviation is close to 2%. However, this observation is based on a blended and weak line (see

TABLE II. Calculated $3d^9\,{}^2D_{5/2,3/2}$ fine-structure intervals $\Delta E(^2D)$ (in cm^{-1}) for Co-like ions with $28 \leqslant Z \leqslant 100$. The Expt.$_{DIR}$ and Expt.$_{IND}$ are directly or indirectly measured fine-structure energies, the MCDHF and RMBPT are from the present calculations, while the Fitted and Semiemp. are fitted and semiempirically estimated transition energies in previously published theoretical work (see text for details).

Z	Ion	Expt.$_{DIR}$	Expt.$_{IND}$	MCDHF[b]	RMBPT[b]	Fitted[e]	Semiemp.
28	Ni^{+}		1506.94[a]	1504			
29	Cu^{2+}		2071.69[a]	2069			
30	Zn^{3+}		2759.1[a]	2758	2541		
31	Ga^{4+}		3583[a]	3583	3433		
32	Ge^{5+}		4560[a]	4560	4448		
33	As^{6+}		5705	5707	5619		
34	Se^{7+}		7037.3	7042	6970		
35	Br^{8+}		8600[a]	8584	8522		
36	Kr^{9+}		10367[a]	10354	10298		
37	Rb^{10+}		12360[a]	12371	12321		
38	Sr^{11+}		14660	14657	14613	14670 ± 10	
39	Y^{12+}		17230	17237	17196	17240 ± 10	
40	Zr^{13+}	20131 ± 1[c]		20132	20093	20125 ± 1.2	
41	Nb^{14+}	23369 ± 5[j]		23367	23331	23363 ± 5	
42	Mo^{15+}	26967 ± 2[c]		26969	26933	26960 ± 1.5	
43	Tc^{16+}			30950	30928	30950 ± 30	
44	Ru^{17+}		35290[d]	35362	35343	35360 ± 40	
45	Rh^{18+}		40200[d]	40222	40205	40230 ± 40	
46	Pd^{19+}		45520[d]	45559	45542	45580 ± 50	
47	Ag^{20+}		51300[d]	51403	51389	51430 ± 50	
48	Cd^{21+}			57785	57771	57810 ± 60	57610[d]
49	In^{22+}			64737	64726	64770 ± 60	64450[d]
50	Sn^{23+}			72293	72281	72340 ± 70	72150[d]
51	Sb^{24+}			80485	80476	80540 ± 80	
52	Te^{25+}			89350	89341	89410 ± 90	
53	I^{26+}			98923	98917	99010 ± 100	
54	Xe^{27+}		109340[a,e]	109242	109236	109340 ± 110	
55	Cs^{28+}			120345	120338	120450 ± 120	120450[a,e]
56	Ba^{29+}		132230[f]	132269	132266	132400 ± 130	
57	La^{30+}		144940[f]	145056	145054	145210 ± 140	
58	Ce^{31+}			158748	158748	158900 ± 160	
59	Pr^{32+}			173386	173386	173560 ± 170	
60	Nd^{33+}		189070[f]	189014	189016	189210 ± 190	
61	Pm^{34+}			205675	205678	205910 ± 200	
62	Sm^{35+}		223630[f]	223416	223420	223680 ± 220	
63	Eu^{36+}			242283	242290	242550 ± 240	
64	Gd^{37+}		262420[f]	262325	262332	262630 ± 260	
65	Tb^{38+}			283590	283600	283940 ± 300	
66	Dy^{39+}		300800[f]	306125	306137	306510 ± 350	
67	Ho^{40+}			329986	329999	330400 ± 400	
68	Er^{41+}			355223	355240	355680 ± 450	355800[f]
69	Tm^{42+}			381889	381908	382390 ± 520	
70	Yb^{43+}			410042	410060	410600 ± 580	410800[f]
71	Lu^{44+}			439731	439752	440350 ± 660	
72	Hf^{45+}	471054 ± 67[g]		471019	471045	471650 ± 740	
73	Ta^{46+}	503956 ± 76[g]		503963	503990	504630 ± 820	
74	W^{47+}	538590 ± 87[a,h]		538621	538651	539350 ± 920	
75	Re^{48+}		576500[i]	575058	575087	575900 ± 1000	
76	Os^{49+}			613327	613362	614200 ± 1100	
77	Ir^{50+}			653500	653540	654400 ± 1300	
78	Pt^{51+}			695638	695681	696600 ± 1400	
79	Au^{52+}	739809 ± 164[g]		739808	739854	740900 ± 1500	
80	Hg^{53+}			786079	786125	787200 ± 1700	
81	Tl^{54+}			834512	834563	835700 ± 1800	
82	Pb^{55+}			885184	885239	886500 ± 2000	
83	Bi^{56+}			938164	938223	939600 ± 2200	

TABLE II. (*Continued.*)

Z	Ion	Expt.$_{\mathrm{DIR}}$	Expt.$_{\mathrm{IND}}$	MCDHF	RMBPT	Fitted[e]	Semiemp.
84	Po^{57+}			993524	993588	995000 ± 2400	
85	At^{58+}			1051344	1051406	1053000 ± 2600	
86	Rn^{59+}			1111685	1111757	1113300 ± 2800	
87	Fr^{60+}			1174637	1174714	1176300 ± 3100	
88	Ra^{61+}			1240273	1240355	1242100 ± 3400	
89	Ac^{62+}			1308673	1308760	1310600 ± 3600	
90	Th^{63+}			1379920	1380008	1381900 ± 3900	
91	Pa^{64+}			1454091	1454186	1456200 ± 4200	
92	U^{65+}			1531278	1531379	1533500 ± 4600	
93	Np^{66+}			1611558	1611670		
94	Pu^{67+}			1695026	1695140		
95	Am^{68+}			1781763	1781880		
96	Cm^{69+}			1871879	1871990		
97	Bk^{70+}			1965416	1965550		
98	Cf^{71+}			2062518	2062650		
99	Es^{72+}			2163258	2163410		
100	Fm^{73+}			2267738	2267890		

[a][66].
[b][30].
[c][37].
[d][2].
[e][35].
[f][31].
[g][41].
[h][42].
[i][33].
[j][38].

TABLE III. Comparisons for the directly measured wavelength (in nm) with the present and previous theoretical data from different methods MCDHF, RMBPT, Fitted, MCDF, RCI, and RCN. For the notation $a(b)$, b is the wavelength uncertainties given in the units of the last significant digit, e.g., 21.229(3) means 21.229 ± 0.003.

Z	Ion	Expt.$_{\mathrm{DIR}}$	MCDHF[a]	RMBPT[a]	Fitted[f]	MCDF[f]	RCI	RCN[h]
40	Zr^{13+}	496.74(3)[b]	496.728	497.6802		500.756[m]		
41	Nb^{14+}	427.91(9)[c]	427.949	428.6200	427.94[g]	431.297[m]		
42	Mo^{15+}	370.81(2)[b]	370.801	371.2864	370.6(7)[i]	373.477[m]		
72	Hf^{45+}	21.229(3)[d]	21.2306	21.2294	21.202(33)	21.315	21.318[d]	20.760
73	Ta^{46+}	19.843(3)[d]	19.8427	19.8417	19.816(32)	19.922	19.923[d]	19.385
74	W^{47+}	18.567(3)[e]	18.5659	18.5649	18.541(32)	18.639	18.640[e]	18.121
					18.51(7)[i]	18.671[j]	18.569[k]	18.6229[l]
						18.649[m]		
79	Au^{52+}	13.517(3)[d]	13.5170	13.5162	13.497(27)	13.569	13.568[d]	13.132
						13.57[m]		

[a]Present results.
[b][37].
[c][38].
[d][41].
[e][42].
[f][35].
[g][2].
[h][46].
[i][31].
[j][43].
[k][45].
[l][44].
[m][36].

TABLE IV. Wavelength λ (nm), probabilities $A^r(s^{-1})$, oscillator strength g_f, and line strength S of the $M1$ transition between $3d^9\,{}^2D_{3/2}$ and ${}^2D_{5/2}$ in Co-like ions with $28 \leqslant Z \leqslant 100$, obtained from the present MCDHF-FCV calculation. Also listed is the lifetime, $\tau_{\rm rad}$ (in s), of the ${}^2D_{3/2}$ state. Notation *a(b)* means $a \times 10^b$.

		MCDHF				
Z	Ion	λ	A^r	g_f	S	$\tau_{\rm rad}$
28	Ni^{+}	6648.70	5.503(−2)	1.459(−07)	2.399	1.82(+01)
29	Cu^{2+}	4833.12	1.433(−1)	2.007(−07)	2.398	6.98(+00)
30	Zn^{3+}	3626.42	3.391(−1)	2.674(−07)	2.398	2.95(+00)
31	Ga^{4+}	2791.32	7.435(−1)	3.474(−07)	2.398	1.34(+00)
32	Ge^{5+}	2192.98	1.533(+0)	4.421(−07)	2.398	6.52(−01)
33	As^{6+}	1752.18	3.005(+0)	5.533(−07)	2.397	3.33(−01)
34	Se^{7+}	1419.99	5.645(+0)	6.826(−07)	2.397	1.77(−01)
35	Br^{8+}	1164.90	1.022(+1)	8.320(−07)	2.397	9.78(−02)
36	Kr^{9+}	965.847	1.794(+1)	1.003(−06)	2.396	5.58(−02)
37	Rb^{10+}	808.361	3.059(+1)	1.199(−06)	2.396	3.27(−02)
38	Sr^{11+}	682.245	5.087(+1)	1.420(−06)	2.396	1.97(−02)
39	Y^{12+}	580.159	8.272(+1)	1.670(−06)	2.395	1.21(−02)
40	Zr^{13+}	496.728	1.316(+2)	1.950(−06)	2.395	7.60(−03)
41	Nb^{14+}	427.949	2.057(+2)	2.263(−06)	2.395	4.86(−03)
42	Mo^{15+}	370.801	3.163(+2)	2.610(−06)	2.394	3.16(−03)
43	Tc^{16+}	323.106	4.785(+2)	2.996(−06)	2.394	2.09(−03)
44	Ru^{17+}	282.790	7.136(+2)	3.422(−06)	2.393	1.40(−03)
45	Rh^{18+}	248.635	1.050(+3)	3.892(−06)	2.393	9.53(−04)
46	Pd^{19+}	219.496	1.526(+3)	4.408(−06)	2.392	6.55(−04)
47	Ag^{20+}	194.542	2.191(+3)	4.972(−06)	2.392	4.56(−04)
48	Cd^{21+}	173.056	3.111(+3)	5.588(−06)	2.391	3.21(−04)
49	In^{22+}	154.471	4.374(+3)	6.259(−06)	2.391	2.29(−04)
50	Sn^{23+}	138.327	6.090(+3)	6.988(−06)	2.390	1.64(−04)
51	Sb^{24+}	124.247	8.402(+3)	7.778(−06)	2.390	1.19(−04)
52	Te^{25+}	111.920	1.149(+4)	8.632(−06)	2.389	8.70(−05)
53	I^{26+}	101.089	1.559(+4)	9.555(−06)	2.389	6.41(−05)
54	Xe^{27+}	91.5400	2.099(+4)	1.055(−05)	2.388	4.76(−05)
55	Cs^{28+}	83.0951	2.806(+4)	1.162(−05)	2.387	3.56(−05)
56	Ba^{29+}	75.6036	3.724(+4)	1.277(−05)	2.387	2.68(−05)
57	La^{30+}	68.9387	4.911(+4)	1.400(−05)	2.386	2.04(−05)
58	Ce^{31+}	62.9929	6.435(+4)	1.531(−05)	2.385	1.55(−05)
59	Pr^{32+}	57.6748	8.382(+4)	1.672(−05)	2.385	1.19(−05)
60	Nd^{33+}	52.9063	1.086(+5)	1.822(−05)	2.384	9.21(−06)
61	Pm^{34+}	48.6204	1.398(+5)	1.982(−05)	2.383	7.15(−06)
62	Sm^{35+}	44.7595	1.792(+5)	2.152(−05)	2.382	5.58(−06)
63	Eu^{36+}	41.2740	2.284(+5)	2.333(−05)	2.382	4.38(−06)
64	Gd^{37+}	38.1207	2.898(+5)	2.526(−05)	2.381	3.45(−06)
65	Tb^{38+}	35.2624	3.660(+5)	2.729(−05)	2.380	2.73(−06)
66	Dy^{39+}	32.6664	4.603(+5)	2.945(−05)	2.379	2.17(−06)
67	Ho^{40+}	30.3043	5.763(+5)	3.174(−05)	2.378	1.74(−06)
68	Er^{41+}	28.1513	7.186(+5)	3.415(−05)	2.377	1.39(−06)
69	Tm^{42+}	26.1856	8.926(+5)	3.670(−05)	2.377	1.12(−06)
70	Yb^{43+}	24.3879	1.104(+6)	3.939(−05)	2.376	9.05(−07)
71	Lu^{44+}	22.7412	1.362(+6)	4.223(−05)	2.375	7.34(−07)
72	Hf^{45+}	21.2306	1.673(+6) 1.65(+6)[a]	4.521(−05)	2.374	5.98(−07)
73	Ta^{46+}	19.8427	2.048(+6) 2.02(+6)[a]	4.836(−05)	2.373	4.88(−07)
74	W^{47+}	18.5659	2.499(+6) 2.47(+6)[b] 2.46(+6)[c]	5.166(−05)	2.372	4.00(−07)
75	Re^{48+}	17.3896	3.040(+6)	5.513(−05)	2.371	3.29(−07)
76	Os^{49+}	16.3045	3.687(+6)	5.878(−05)	2.370	2.71(−07)

TABLE IV. (*Continued.*)

		MCDHF				
Z	Ion	λ	A^r	g_f	S	τ_{rad}
77	Ir^{50+}	15.3022	4.458(+6)	6.260(−05)	2.369	2.24(−07)
78	Pt^{51+}	14.3753	5.375(+6)	6.660(−05)	2.368	1.86(−07)
79	Au^{52+}	13.5170	6.462(+6)	7.080(−05)	2.367	1.55(−07)
			6.38(+6)[a]			
80	Hg^{53+}	12.7214	7.748(+6)	7.519(−05)	2.365	1.29(−07)
81	Tl^{54+}	11.9831	9.266(+6)	7.979(−05)	2.364	1.08(−07)
82	Pb^{55+}	11.2971	1.105(+7)	8.459(−05)	2.363	9.04(−08)
83	Bi^{56+}	10.6591	1.315(+7)	8.961(−05)	2.362	7.60(−08)
84	Po^{57+}	10.0652	1.561(+7)	9.485(−05)	2.361	6.40(−08)
85	At^{58+}	9.51168	1.849(+7)	1.003(−04)	2.360	5.41(−08)
86	Rn^{59+}	8.9954	2.185(+7)	1.060(−04)	2.358	4.58(−08)
87	Fr^{60+}	8.5133	2.576(+7)	1.120(−04)	2.357	3.88(−08)
88	Ra^{61+}	8.0627	3.031(+7)	1.182(−04)	2.356	3.30(−08)
89	Ac^{62+}	7.6413	3.558(+7)	1.246(−04)	2.354	2.81(−08)
90	Th^{63+}	7.2468	4.169(+7)	1.313(−04)	2.353	2.40(−08)
91	Pa^{64+}	6.8772	4.876(+7)	1.383(−04)	2.352	2.05(−08)
92	U^{65+}	6.5305	5.691(+7)	1.455(−04)	2.350	1.76(−08)
93	Np^{66+}	6.2052	6.630(+7)	1.531(−04)	2.349	1.51(−08)
94	Pu^{67+}	5.8996	7.709(+7)	1.609(−04)	2.348	1.30(−08)
95	Am^{68+}	5.6124	8.949(+7)	1.690(−04)	2.346	1.12(−08)
96	Cm^{69+}	5.3422	1.037(+8)	1.775(−04)	2.345	9.64(−09)
97	Bk^{70+}	5.0880	1.200(+8)	1.862(−04)	2.343	8.33(−09)
98	Cf^{71+}	4.8484	1.385(+8)	1.953(−04)	2.342	7.21(−09)
99	Es^{72+}	4.6227	1.597(+8)	2.047(−04)	2.340	6.26(−09)
100	Fm^{73+}	4.4097	1.839(+8)	2.144(−04)	2.338	5.43(−09)

[a][41].
[b][42].
[c][43].

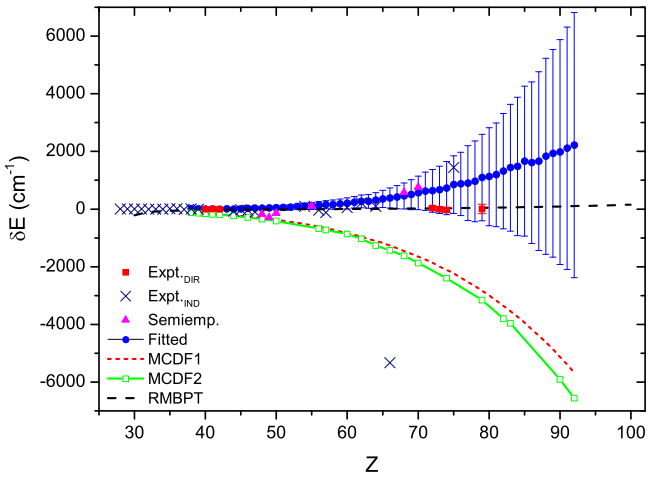

FIG. 5. Comparison of the $3d^9\ ^2D_{3/2} \rightarrow\ ^2D_{5/2}$ fine-structure splitting from various computations and experiments with the results of the present MCDHF calculations as a function of nuclear charge Z. The Expt.$_{DIR}$, Expt.$_{IND}$, Semiemp., and Fitted, respectively, represent directly measured, indirectly measured, semiempirically computed, and fitted transition energies (see text). The latter are given with error bars. While the MCDF1 [35], MCDF2 [36], and RMBPT are, respectively, from earlier and present calculations (see text).

Reader [31]) and probably not correct. Second, the observation for Re^{48+} ($Z = 75$) is probably also incorrect, as pointed out by Seely *et al.* [33].

The fine structures of the semiempirical results for Er^{41+}, Yb^{43+} ($Z = 68, 70$) slightly deviate from our calculations, but are based on predictions by Reader [31] from isoelectronic extrapolations of known experimental fine-structure intervals and are therefore less accurate.

The results labeled "Fitted" in Table II and Fig. 5 are semiempirical fitted predictions of the fine structure by Ekberg *et al.* [35]. The trend for these predictions deviates from ours, but our results are always within the estimated error bars of the fitted value.

On the theoretical side, we present in Fig. 5 not only the deviation from our MCDHF results of our present RMBPT results but also the deviation of the two earlier *ab initio* calculations by Ekberg *et al.* [35] and Chen [36], using an earlier version of the MCDF computer program by Grant *et al.* [53] marked as MCDF1 and MCDF2, respectively. It is clear that the present MCDHF-FCV is significantly more accurate than earlier calculations. We also note that the modified RMBPT converges to the present MCDHF results for higher Z, but is less accurate for the low-Z end of the sequence, where the correlation effects are more important.

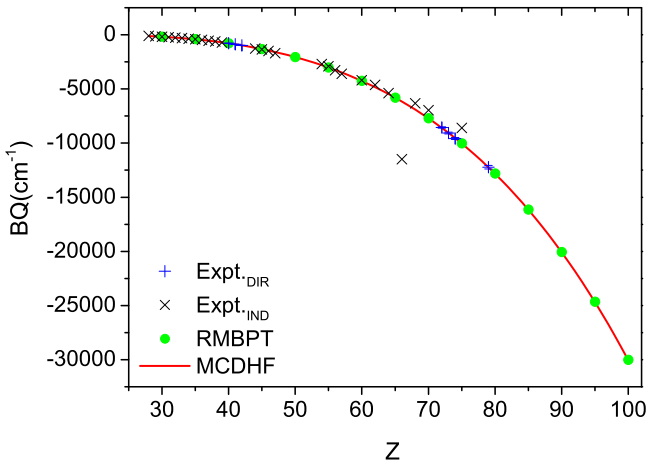

FIG. 6. Contributions of Breit interaction and QED (BQ) effects to the $3d^2\,{}^2D$ fine-structure energy. The Expt.$_{\rm DIR}$ and Expt.$_{\rm IND}$ represent results from direct and indirect measurements, respectively (see text).

Wavelengths from direct measurements [37,38,41,42] are reported in Table III and compared to theoretical results from both our present MCDHF calculations as well as RMBPT and earlier theoretical works [2,31,35,36,41–46]. It is obvious that our results are very accurate and fall well within the error bars of the measured values. The RMBPT wavelengths for higher-Z ions (Hf^{45+}, Ta^{46+}, W^{47+}, Au^{52+}) agree within the experimental uncertainties, but for the lower-Z ions there exist differences of about 0.15%. The fitted results by Ekberg *et al.* [35] are close to the experimental ones for Nb^{14+}, but lower than the measured ones by 0.13% for the four higher-Z ions. For the *ab initio* wavelengths from the MCDF [35,36,43], RCI [41,42], and semirelativistic Cowan code (RCN) [46] calculations, the differences with measured ones can reach up to 0.9, 0.4, and 2.8%, respectively. The newest RCI wavelength for W^{47+} calculated by Clementson *et al.* [45] using the FAC code also falls within the experimental error bars.

The high accuracy of the present results makes it possible to investigate the representation of the combined BQ effects. If we assume that our representation of correlation is converged, we can define the difference between the experimental energy splitting and our results without including Breit and QED (labeled DC in Table I) as representing the combined BQ effects. We display this as a function of Z in Fig. 6, together with our MCDHF and RMBPT representation of these effects. It is somewhat surprising that both the MCDHF and RMBPT representations of the BQ effect seem to be accurate, in spite of the approximate treatment.

In Table IV, we give the computed wavelength (λ, in nm), rates (A^r_{ji}, in s^{-1}), and line strengths (S, in a.u.) for the magnetic dipole ($M1$) transition $3d^9\,{}^2D_{3/2} \rightarrow {}^2D_{5/2}$ from our MCDHF calculations. The previously published $M1$ transition rates for Hf^{45+}, Ta^{46+}, W^{47+}, and Au^{52+} ions obtained by means of RCI [41,42] and MCDF [43] approaches are also listed in Table IV. All of these rates are lower than the present MCDHF ones by 1.3% on average.

The lifetime ($\tau_{\rm rad}$, in s) of state ${}^2D_{3/2}$ is also given in Table IV, as obtained from the $M1$ and the electric quadrupole ($E2$) transitions. However, the $E2$ transition rates are not included in the table, since their contribution is negligible. In the lower-Z part, the $M1$ transition rate is five orders of magnitude larger than the $E2$ transition. Although according to the Z dependence of transition properties [67] the $E2$ transition rate (proportional to Z^{16}) increases more rapidly than the $M1$ transition rate (proportional to Z^{12}) along the isoelectronic sequence, it is still smaller than the $M1$ rate by three orders of magnitude for high Z.

The line strength (S) of the $M1$ transition between the fine-structure levels in $3d^9\,{}^2D$ in the nonrelativistic single-configuration limit gives a value of 2.4, independent of the radial functions involved [68]. This is reproduced in the present MCDHF calculations, as seen from Table IV. In fact, we have also calculated the line strength within the RMBPT method. It is found that the RMBPT S value is lower than the MCDHF one by over 10% for ions with $Z \leqslant 35$ (up to 25% for Zn^{3+}), though there is a better agreement for $Z \geqslant 50$ (to within 3%). This indicates an error in the calculation of line strength for the $M1$ transition in the RMBPT implementation within the FAC code, which is presently under investigation. We recommend caution in the use of the results for $M1$ transitions from this code, until this is corrected.

VI. CONCLUSIONS

In this work, we have presented a detailed treatment of electron-correlation, Breit interaction, and QED effects for the $3d^9$ ground configurations of Co-like ions by using two state-of-the-art methods, MCDHF and RMBPT. With the MCDHF approach, it was shown that the deep core-valence correlations with $2p$ rather than $3p$ and $2s$ rather than $3s$ are the dominant contributors. All of these correlations should be included in the calculation to reach spectroscopic accuracy. The Breit interaction is the dominating correction to the fine-structure splitting energy for the whole sequence.

By comparing the detailed differences of correlation, Breit, and QED effects between the MCDHF and RMBPT, we corrected for the omitted $j \geqslant 5/2$ contributions to the self-energy in the implementation of the RMBPT method within the FAC code. These contributions are important for the calculations of spectroscopic accuracy. We also discovered a possible error in the FAC-code treatment of $M1$ rates. The RMBPT code give less accurate results for the transition energy for low-Z ions, but the agreement with the MCDHF is within 0.01% for $Z > 50$.

The present MCDHF fine-structure splittings have excellent agreement with all directly observed ones, with estimated uncertainties of 0.02%. However, the RMBPT can only reproduce these to within the experimental uncertainties for higher-Z ions. The previously published *ab initio* results and fitted data diverge from the present MCDHF and RMBPT results along the isoelectronic sequence. We hope that our results will be further checked by new highly accurate experiments, especially for mid-Z ($50 \leqslant Z \leqslant 60$) and high-$Z$ ($Z > 80$) value.

Our theoretical results are orders of magnitude more accurate than earlier theoretical results and can be used to test Breit and QED effects, especially for high-Z elements. The methods adopted here will also comprise an important first

step in future investigations of other multielectron sequences, such as Rh-like ($4d^9$), Fe-like ($3d^8$), and Mn-like ($3d^7$) ions.

ACKNOWLEDGMENTS

This work was supported by NSAF under Grant No. 11076009, National Natural Science Foundation of China under Grant No. 11374062, and Chinese Association of Atomic and Molecular Data. It was also partially supported by the Chinese National Fusion Project for ITER under Grant No. 2015GB117000 and Shanghai Leading Academic Discipline Project under Grant No. B107. X.L.G. would especially like to thank the Swedish Research Council 2015-04842, the International Exchange Program Fund of Doctoral Student under the Fudan University Graduate School, and the Nordic Centre at Fudan University for supporting her exchange study in Lund university.

[1] M. Eidelsberg, F. Crifo-Magnant, and C. J. Zeippen, Forbidden lines in hot astronomical sources, Astro. Astrophys. Suppl. Ser. **43**, 455 (1981).

[2] B. Edlén, Forbidden lines in hot plasmas, Phys. Scr. **1984**, 5 (1984).

[3] V. Kaufman and J. Sugar, Forbidden lines in ns^2np^k ground configurations and *nsnp* excited configurations of beryllium through molybdenum atoms and ions, J. Phys. Chem. Ref. Data **15**, 321 (1986).

[4] E. Biémont and C. J. Zeippen, Probabilities for forbidden transitions in atoms and ions: 1989-1995. A commented bibliography, Phys. Scr. **1996**, 192 (1996).

[5] V. I. Yudin, A. V. Taichenachev, and A. Derevianko, Magnetic-Dipole Transitions in Highly Charged Ions as a Basis of Ultraprecise Optical Clocks, Phys. Rev. Lett. **113**, 233003 (2014).

[6] J. C. Berengut, V. A. Dzuba, V. V. Flambaum, and A. Ong, Electron-Hole Transitions in Multiply Charged Ions for Precision Laser Spectroscopy and Searching for Variations in α, Phys. Rev. Lett. **106**, 210802 (2011).

[7] S. G. Karshenboim, Precision physics of simple atoms: QED tests, nuclear structure and fundamental constants, Phys. Rep. **422**, 1 (2005).

[8] A. N. Artemyev, V. M. Shabaev, I. I. Tupitsyn, G. Plunien, and V. A. Yerokhin, QED Calculation of the $2p_{3/2} - 2p_{1/2}$ Transition Energy in Boronlike Argon, Phys. Rev. Lett. **98**, 173004 (2007).

[9] B. Edlén, Die Deutung der Emissionslinien im Spektrum der Sonnenkorona. Mit 6 Abbildungen, Z. Astrophysik **22**, 30 (1943).

[10] Y. K. Kim, D. H. Baik, P. Indelicato, and J. P. Desclaux, Resonance transition energies of Li-, Na-, and Cu-like ions, Phys. Rev. A **44**, 148 (1991).

[11] S. A. Blundell, Calculations of the screened self-energy and vacuum polarization in Li-like, Na-like, and Cu-like ions, Phys. Rev. A **47**, 1790 (1993).

[12] A. Lapierre, U. D. Jentschura, J. R. Crespo López-Urrutia, J. Braun, G. Brenner, H. Bruhns, D. Fischer, A. J. González Martínez, Z. Harman, W. R. Johnson, C. H. Keitel, V. Mironov, C. J. Osborne, G. Sikler, R. Soria Orts, V. Shabaev, H. Tawara, I. I. Tupitsyn, J. Ullrich, and A. Volotka, Relativistic Electron Correlation, Quantum Electrodynamics, and the Lifetime of the $1s^22s^22p^2P^o_{3/2}$ Level in Boronlike Argon, Phys. Rev. Lett. **95**, 183001 (2005).

[13] V. Mäckel, R. Klawitter, G. Brenner, J. R. Crespo López-Urrutia, and J. Ullrich, Laser Spectroscopy on Forbidden Transitions in Trapped Highly Charged Ar^{13+} Ions, Phys. Rev. Lett. **107**, 143002 (2011).

[14] A. N. Artemyev, V. M. Shabaev, I. I. Tupitsyn, G. Plunien, A. Surzhykov, and S. Fritzsche, Ab initio calculations of the $2p_{3/2} - 2p_{1/2}$ fine-structure splitting in boronlike ions, Phys. Rev. A **88**, 032518 (2013).

[15] G. Brenner, J. R. Crespo López-Urrutia, Z. Harman, P. H. Mokler, and J. Ullrich, Lifetime determination of the FeXIV $3s^23p^2P^o_{3/2}$ metastable level, Phys. Rev. A **75**, 032504 (2007).

[16] L. H. Hao, G. Jiang, and H. J. Hou, Effects of valence-valence, core-valence, and core-core correlations on the fine-structure energy levels in Al-like ions, Phys. Rev. A **81**, 022502 (2010).

[17] M. J. Vilkas and Y. Ishikawa, Relativistic multireference many-body perturbation-theory calculations on the multiple openshell states in siliconlike Ar and aluminumlike Fe ions, Phys. Rev. A **68**, 012503 (2003).

[18] U. I. Safronova, C. Namba, J. R. Albritton, W. R. Johnson, and M. S. Safronova, Relativistic many-body calculations of energies of $n = 3$ states in aluminumlike ions, Phys. Rev. A **65**, 022507 (2002).

[19] M. S. Safronova and U. I. Safronova, Relativistic many-body calculation of energies, oscillator strengths, transition rates, and lifetimes of Sc III ion, Phys. Rev. A **85**, 022504 (2012).

[20] L. H. Hao and G. Jiang, Energy levels, transition rates, and line strengths of B-like ions, Phys. Rev. A **83**, 012511 (2011).

[21] C. Thierfelder and P. Schwerdtfeger, Quantum electrodynamic corrections for the valence shell in heavy many-electron atoms, Phys. Rev. A **82**, 062503 (2010).

[22] M. A. Ali and Y. K. Kim, Improved calculation of fine-structure splittings in the ground state of potassiumlike ions, J. Opt. Soc. Am. B **9**, 185 (1992).

[23] Z. Fei, R. Zhao, Z. Shi, J. Xiao, M. Qiu, J. Grumer, M. Andersson, T. Brage, R. Hutton, and Y. Zou, Experimental and theoretical study of the ground-state M1 transition in Ag-like tungsten, Phys. Rev. A **86**, 062501 (2012).

[24] J. Grumer, R. Zhao, T. Brage, W. Li, S. Huldt, R. Hutton, and Y. Zou, Coronal lines and the importance of deep-core-valence correlation in Ag-like ions, Phys. Rev. A **89**, 062511 (2014).

[25] L. J. Curtis, J. Reader, S. Goldsmith, B. Denne, and E. Hinnov, $4s^24p^2P$ intervals in the Ga isoelectronic sequence from Rb^{6+} to In^{18+}, Phys. Rev. A **29**, 2248 (1984).

[26] B. Edlén, Spectra of highly ionized atoms, Physica **13**, 545 (1947).

[27] J. F. Seely, J. O. Ekberg, C. M. Brown, U. Feldman, W. E. Behring, J. Reader, and M. C. Richardson, Laser-Produced Spectra and QED Effects for Fe-, Co-, Cu-, and Zn-like Ions of Au, Pb, Bi, Th, and U, Phys. Rev. Lett. **57**, 2924 (1986).

[28] E. Alexander, M. Even-Zohar, B. S. Fraenkel, and S. Goldsmith, Classification of Transitions in the EUV Spectra of Y IX-XIII,

Zr X-XIV, Nb XI-XV, and Mo XII-XVI, J. Opt. Soc. Am. **61**, 508 (1971).
[29] P. G. Burkhalter, J. Reader, and R. D. Cowan, Spectra of Mo XIII-XVIII from a laser-produced plasma and a low-inductance vacuum spark, J. Opt. Soc. Am. **70**, 912 (1980).
[30] A. N. Ryabtsev and J. Reader, Spectra of the cobaltlike ions Sr XII, Y XIII, Zr XIV, Nb XV, and Mo XVI, J. Opt. Soc. Am. **72**, 710 (1982).
[31] J. Reader, $3p^6 3d^9 - 3p^5 3d^{10}$ transitions in cobaltlike ions from Ba^{29+} to Yb^{43+}, J. Opt. Soc. Am. **73**, 63 (1983).
[32] J.-F. Wyart, M. Klapisch, J.-L. Schwob, and N. Schweitzer, The $3d^9 - 3d^8 4p$ Transitions in the Spectra of Highly-Ionized Elements Yttrium to Silver (Y XIII-Ag XXI), Phys. Scr. **26**, 141 (1982).
[33] J. F. Seely, C. M. Brown, and W. E. Behring, Transitions in Fe-, Co-, Cu-, and Zn-like ions of W and Re, J. Opt. Soc. Am. B **6**, 3 (1989).
[34] J. Clementson, P. Beiersdorfer, G. V. Brown, and M. F. Gu, Spectroscopy of M-shell x-ray transitions in Zn-like through Co-like W, Phys. Scr. **81**, 015301 (2010).
[35] J. O. Ekberg, U. Feldman, J. F. Seely, C. M. Brown, J. Reader, and N. Acquista, $3p^6 3d^9 - 3p^5 3d^{10}$ transitions of cobaltlike ions from Sr^{11+} to U^{65+}, J. Opt. Soc. Am. B **4**, 1913 (1987).
[36] M. H. Chen, Wavelengths of the $3p - 3d$ transitions of the Co-like ions, Phys. Rev. A **36**, 665 (1987).
[37] S. Suckewer, E. Hinnov, S. Cohen, M. Finkenthal, and K. Sato, Identification of magnetic dipole lines above 2000 Å in several highly ionized Mo and Zr ions on the PLT tokamak, Phys. Rev. A **26**, 1161 (1982).
[38] M. H. Prior, Forbidden lines from highly charged, metastable ion beams, J. Opt. Soc. Am. B **4**, 144 (1987).
[39] J. M. Pomeroy, J. N. Tan, Y. Ralchenko, J. Reader, and J. D. Gillaspy, Spectra of W^{39+} C W^{47+} in the 12C20 nm region observed with an EBIT light source, J. Phys. B **40**, 3861 (2007).
[40] I. N. Draganić, Y. Ralchenko, and J. Reader, EUV spectral lines of highly-charged Hf, Ta and Au ions observed with an electron beam ion trap, J. Phys. B **44**, 025001 (2011).
[41] D. Osin, J. D. Gillaspy, J. Reader, and Yu. Ralchenko, EUV magnetic-dipole lines from highly-charged high-Z ions with an open $3d$ shell, Eur. Phys. J. D **66**, 286 (2012).
[42] Yu. Ralchenko, I. N. Draganić, D. Osin, J. D. Gillaspy, and J. Reader, Spectroscopy of diagnostically important magnetic-dipole lines in highly charged $3d^n$ ions of tungsten, Phys. Rev. A **83**, 032517 (2011).
[43] P. Quinet, Dirac-Fock calculations of forbidden transitions within the $3p^k$ and $3d^k$ ground configurations of highly charged tungsten ions (W^{47+}-W^{61+}), J. Phys. B **44**, 195007 (2011).
[44] K. B. Fournier, Atomic data and spectral line Intensities for highly ionized tungsetn (Co-like W^{47+} to Rb-like W^{37+}) in a high-temperature, low-density plasma, At. Data Nucl. Data Tables **68**, 1 (1998).
[45] J. Clementson, P. Beiersdorfer, T. Brage, and M. F. Gu, Atomic data and theoretical X-ray spectra of Ge-like through V-like W ions, At. Data Nucl. Data Tables **100**, 577 (2014).
[46] J. Reader, J. D. Gillaspy, D. Osin, and Yu. Ralchenko, Magnetic-dipole transitions in tungsten and other heavy elements observed with the NIST EBIT, AIP Conf. Proc. **1438**, 86 (2012).
[47] X. L. Guo, M. Huang, J. Yan, S. Li, R. Si, C. Y. Li, C. Y. Chen, Y. S. Wang, and Y. M. Zou, Relativistic many-body calculations on wavelengths and transition probabilities for forbidden transitions within the $3d^k$ ground configurations in Co- through K-like ions of hafnium, tantalum, tungsten and gold, J. Phys. B **48**, 144020 (2015).
[48] M. F. Gu, The flexible atomic code, Can. J. Phys. **86**, 675 (2008).
[49] M. F. Gu, T. Holczer, E. Behar, and S. M. Kahn, Inner-shell absorption lines of Fe VI-Fe XVI: A many-body perturbation theory approach, Astrophys. J. **641**, 1227 (2006).
[50] M. F. Gu, Many-body perturbation theory wavelengths of High-n X-Ray transitions of Fe and Ni L-shell ions, Astrophys. J. Suppl. Ser **169**, 154 (2007).
[51] P. Jonsson, X. He, C. Froese Fischer, and I. P. Grant, The grasp2K relativistic atomic structure package, Comput. Phys. Commun. **177**, 597 (2007).
[52] P. Jönsson, G. Gaigalas, J. Bieroń, C. Froese Fischer, and I. P. Grant, New version: Grasp2K relativistic atomic structure package, Comput. Phys. Commun. **184**, 2197 (2013).
[53] I. P. Grant, B. J. McKenzie, P. H. Norrington, D. F. Mayers, and N. C. Pyper, An atomic multiconfigurational Dirac-Fock package, Comput. Phys. Commun. **21**, 207 (1980).
[54] J. Olsen, B. O. Roos, P. Jørgensen, and H. Jørgen Aa. Jensen, Determinant based configuration interaction algorithms for complete and restricted configuration interaction spaces, J. Chem. Phys. **89**, 2185 (1988).
[55] P. J. Mohr, Self-energy of the $n = 2$ states in a strong Coulomb field, Phys. Rev. A **26**, 2338 (1982).
[56] B. J. McKenzie, I. P. Grant, and P. H. Norrington, A program to calculate transverse Breit and QED corrections to energy levels in a multiconfiguration Dirac-Fock environment, Comput. Phys. Commun. **21**, 233 (1980).
[57] Z. J. Fei, W. X. Li, J. Grumer, Z. Shi, R. Zhao, T. Brage, S. Huldt, K. Yao, R. Hutton, and Y. Zou, Forbidden-line spectroscopy of the ground-state configuration of Cd-like W, Phys. Rev. A **90**, 052517 (2014).
[58] K. Wang, D. F. Li, H. T. Liu, X. Y. Han, B. Duan, C. Y. Li, J. G. Li, X. L. Guo, C. Y. Chen, and J. Yan, Systematic calculations of energy levels and transition rates of C-like Ions with $Z = 13 - 36$, Astrophys. J. Suppl. Ser. **215**, 26 (2014).
[59] R. Si, X. L. Guo, J. Yan, C. Y. Li, S. Li, M. Huang, C. Y. Chen, Y. S. Wang, and Y. M. Zou, Energy levels and oscillator strengths for Mg-like copper, J. Quant. Spectrosc. Radiat. Transfer **163**, 7 (2015).
[60] K. Wang, X. L. Guo, H. T. Liu, D. F. Li, F. Y. Long, X. Y. Han, B. Duan, J. G. Li, M. Huang, Y. S. Wang, R. Hutton, Y. M. Zou, J. L. Zeng, C. Y. Chen, and J. Yan, Systematic calculations of energy levels and calculations of energy levels and transition rates of Be-like ions with $Z = 10 - 30$ using a combined configuration interaction and many-body perturbation theory approach, Astrophys. J. Suppl. Ser. **218**, 16 (2015).
[61] J. Sucher, Foundations of the relativistic theory of many-electron atoms, Phys. Rev. A **22**, 348 (1980).
[62] T. Brage and C. F. Fischer, Systematic calculations of correlation in complex ions, Phys. Scr. **47**, 18 (1993).
[63] C. F. Fischer and G. Gaigalas, Multiconfiguration Dirac-Hartree-Fock energy levels and transition probabilities for W XXXVIII, Phys. Rev. A **85**, 042501 (2012).
[64] P. J. Mohr, Lamb Shift in a Strong Coulomb Potential, Phys. Rev. Lett. **34**, 1050 (1975).

[65] P. J. Mohr and Y. K. Kim, Quantum defect theory. XIII. Radiative transitions, Phys. Rev. A **45**, 2727 (1992).

[66] A. Kramida, Yu. Ralchenko, J. Reader, and NIST ASD Team, NIST Atomic Spectra Database (ver. 5.1), http://physics.nist.gov/asd, National Institute of Standards and Technology, Gaithersburg, MD, 2013.

[67] C. F. Fischer, T. Brage, and P. Jonsson, *Computational Atomic Structure—An MCHF Approach* (Institute of Physics, University of Reading, Berkshire, 1997).

[68] R. D. Cowan, *The Theory of Atomic Structure and Spectra* (University of California, Berkeley, 1981).